COBEM UBERLÂNDIA 2019

ABCM Associação Brasileira de Engenharia e Ciências Mecânicas

25th ABCM International Congress of Mechanical Engineering
October 20-25, 2019, Uberlândia, MG, Brazil

COB-2019-0019
MATHEMATICAL MODELING OF THE FLAME TEMPERATURE OF NATURAL GAS THROUGH METHANE CONCENTRATION, TEMPERATURE AND EXCESS AIR IN REHEATING FURNACES

Diego Jhovanny Mariños Rosado
Samir Boset Rojas Chávez
João Andrade de Carvalho Jr
São Paulo State University, Campus of Guaratinguetá, Av. Ariberto P. Cunha, 333, Guaratinguetá, SP, CEP 12510-410, Brazil
diego.marinos@hotmail.com; samir.rojaschavez@hotmail.com; ja.carvalho@unesp.br

Roberto Carlos Chucuya Huallpachoque
National University of Santa, Department of Energy and Physics, Av. Pacífico 508. Chimbote, Ancash, Peru.
roberto_chucuya@yahoo.es

Abstract. *The objective of this article was to develop a mathematical model for the determination of the adiabatic flame temperature in reheating furnaces, based on three independent variables such as the concentration of methane (CH_4) in the preparation of the fuel (natural gas), excess air (α) and air temperature (T_{air}).*
The developed model applied the factorial experiment tool 2^3 and the statistical analysis. The accuracy of the model was tested in terms of the square correlation coefficient (R^2). Finally, with the mathematical equation obtained, three cases were developed to obtain the maximum adiabatic flame temperature, varying two of the three initial factors (CH_4, α and T_{air}) and keeping the third factor constant in each case.
It was evidenced that the adiabatic flame temperature obtained by the mathematical model is equal in magnitude to those obtained by the stoichiometric reaction of the fuel, this was determined by the coefficient of correlation to the square (R^2) that was equal to 1. In the same way, the maximum adiabatic flame temperature was obtained when the methane concentration in the fuel preparation is 70%, the excess air is 20% and the air is preheated to the temperature of 873K.

Keywords: *adiabatic flame temperature, factorial experiments, industrial furnaces, mathematical modeling, steel industry.*

1. INTRODUCTION

The steel industry has made great strides in steel production (Lu *et al.*, 2016), product structure (Barmatov *et al.*, 2017), energy economy (Yang *et al.*, 2017), and is an important industry in world economic development (Ma *et al.*, 2014). The rapid development of the steel industry is accompanied by huge energy consumption, which takes place in Brazil, China, Europe and around the world (Chen *et al.*, 2018). The energy consumption of the steel industry represents between 10% and 15% of the total energy consumption in the world (Chen *et al.*, 2018). Reheating furnaces are used in the steel industry to heat slabs, parts, forging tasks and for the heat treatment of rolled steel (Andreas, 2011), in the same way, the iron undergoes several thermal, mechanical or thermomechanical processes suitable for industrial applications (Casal *et al.*, 2015). The energy consumption of reheating furnaces depends to a large extent on a number of factors, such as steel grade, furnace size, rate of production, desired reheating temperature and temperature uniformity. However, there is a strong contradiction between the high energy consumption and the traditional source of energy increasingly exhausted. With the rapid growth of energy consumption not only increased the cost of the industry (Rasul *et al.*, 2007), also increased emissions of pollutants into the environment. The steel industry is known as one of the main sectors of CO_2 emissions in the world, representing approximately 7% of the total (An *et al.*, 2018), emitting on average 1.8 tons of CO_2 per ton of steel produced (Han *et al.*, 2012); with China being the world's largest CO_2 emitter, with around 10Gt CO_2 per year (Oliveira *et al.*, 2014) and South Korea is the third largest emitter of CO_2 that produces approximately 90 million tons of CO_2 per year (Han *et al.*, 2011). Among other polluting gases in this industry, we have NO_x (Gan *et al.*, 2016), and SO_2 (Chun *et al.*, 2017).

The ability to accurately determine the temperature of steel is of great importance in different areas. In the steel industry, it is necessary to keep the temperature distribution as uniform as possible to ensure good product quality (Landfahrer *et al.*, 2018). In other areas, such as cutting processes, the ability to detect and avoid temperature peaks can extend tool life (Husmann *et al.*, 2016). The heat flow can also be measured using an infrared camera (Švantner *et al.*, 2012). In general, measuring the temperature is not an easy task; therefore, several measurement methods have been developed for this purpose (Alves *et al.*, 2018). Thermocouples represent the most commonly used method of contact measurement. In some cases, however, it is not possible to use thermocouples and, instead, a non-contact method is widely used. Non-contact methods include the use of infrared cameras, radiation pyrometers and materials with known melting points or the ability to change their microstructure. Such techniques are mostly fast, accurate and economical. In the steel industry, the temperature of the steel entering and leaving the kiln is mainly recorded by means of radiation pyrometers.

Control the adiabatic flame temperature (maximum theoretical temperature that can be reached in the combustion (Wang *et al.*, 2018; Wu *et al.*, 2018) is of great importance for the steel industry, because through the temperature of the flame it is possible to regulate the temperature of certain materials that only need heat treatment so as not to exceed the metallurgical limit and cause the smelting (Stelzner *et al.*, 2017). Many methods have been developed to control the flame (Hindasageri *et al.*, 2014), the most common is oxygen enrichment, preheating the air (Caillat, 2017), preheating the fuel and to reduce the combustion temperature, excess air is used (Strobel *et al.*, 2018). Several models have been studied to improve the efficiency of the reheating furnace and obtain better control of the flame temperature (Emadi *et al.*, 2014).

The objective of this work is to propose a mathematical model to determine the adiabatic flame temperature in a simple way, knowing the variables and the most important parameters, such as methane concentration in the fuel for its preparation, excess air and air temperature. The equation obtained from the model will theoretically evaluate the presented parameters and predict the adiabatic flame behavior. For this purpose, the factorial experiment tool 2^3 will be used and the statistical analysis (Montgomery, 2001). This tool defines the effects of the factors, the global variance without replicates, the experimental error, the tests of significance and the coding of the variables. The mathematical model is validated using Microsoft Excel software. The mathematical equation will be developed three cases, varying two of the three initial variables (methane concentration, excess air and air temperature) and keeping the third variable constant in each case. This allows to obtain an adiabatic flame temperature distribution to facilitate its study, establishing the necessary temperature to reach in the reheating furnace.

2. METHODOLOGY

2.1. Review of the factorial experiment tool 2^3

2.1.1. Effects of factors

It is defined as the difference of the mean of the output variable with signal (+) and signal (-), which represent the symbols assigned to the input variables in each case.

$$E = \bar{Y}\,(+) - \bar{Y}\,\,(-) \tag{1}$$

E are the effects that can be first, second and third order, $\bar{Y}\,(+)$ and $\bar{Y}\,(-)$ represent the mean of the output variables (response) as a function of the input variables.

2.1.2. Global variance without replicates

It is the relationship between the square of the interaction effects of order greater than two and the number of interactions of order greater than two.

$$S_P{}^2 = \frac{\sum(interaction\ effects\ of\ order>2\,)^2}{Number\ of\ order\ interactions>2} \tag{2}$$

$S_P{}^2$ is the global variance without replicas assigned when there is an output variable for each case.

2.1.3. Experimental error

S_P is the experimental error defined as the square root of the non-replicated global variance.

$$S_P = \sqrt{S_P{}^2} \tag{3}$$

2.1.4. Significance test

It is the relation of the absolute value of the effects of first, second and third order, with the experimental error.

$$t_{cal} = \frac{|Effect|}{S_P} \tag{4}$$

t_{cal} is the test of significance that is related to the critical test (t_{cri}) obtained with a certain degree of freedom and a level of significance. When $t_{cal} \geq t_{cri}$ the result is significant, but when $t_{cal} < t_{cri}$ the result is not significant. Two-factor tests that are significant will be evaluated through interaction graphs to determine if there is a relationship between the variables evaluated.

2.1.5. Coded variable

It is the coding of the independent variables (input) to facilitate their assembly in the mathematical equation obtained from the application of the factorial tool 2^3. The coded variables are between -1 and +1, facilitating the visualization in the answers.

$$VC_i = \frac{2X_i-(X_{i-min}+X_{i-max})}{(X_{i-min}-X_{i-max})} \tag{5}$$

VC_i is the coded variable, X_i is the value of the input variable (A, B or C), X_{i-min} and X_{i-max} are the values of the minimum and maximum variables, respectively.

The main advantages of using coded variables to fit polynomial models are as follows: Increase precision in determining model coefficients, improve interpretation and visualization of model coefficients, and enable analysis through the confidentiality of operational data.

2.1.6. Mathematical model

It is the final result of the application of the factorial experiment tool 2^3 (Montgomery DC, 2001). The mathematical model obtained is executed with the coding of the input variables and their effects, as shown in Eq. (6).

$$Y = media + \frac{E_A}{2}(VC_A) + \frac{E_B}{2}(VC_B) + \frac{E_C}{2}(VC_C) + \frac{E_{AB}}{2}(VC_A * VC_B) + \frac{E_{AC}}{2}(VC_A * VC_C) + \frac{E_{BC}}{2}(VC_B * VC_C) + \frac{E_{ABC}}{2}(VC_A * VC_B * VC_C) \tag{6}$$

Y is the response variable, E_i are the effects of first, second and third order, and VC_i is the encoded variable of the input factors.

2.2. Thermodynamic properties and stoichiometric reaction

The adiabatic flame temperature obtained by the combustion of natural gas in industrial furnaces aims to propose solutions to problems identified in the combustion due to the inefficiency of the flame that prevents a good transfer of heat, a correct burning of the fuel and this leads to the increase of the generation of pollutants, causing instability of the furnace, in addition to regulating the temperature of certain materials that only need heat treatment to not exceed the metallurgical limit and cause the smelting.

The adiabatic flame temperature is determined by varying the methane concentration in the natural gas composition, the percentage of excess air and the air temperature, as shown in Tab. 1.

Table 1. Minimum and maximum range of the operational variables of the natural gas combustion process.

	Methane - CH_4 (%)	Excess air - α (%)	Air temperature - T_{air} (K)
Minimum (-1)	70	20	298
Maximum (+1)	90	80	873

The model applies the concentration of methane (CH_4) and automatically determines the concentration of ethane (C_2H_6) to complete the 100% that are required in the stoichiometric reaction and also for the combustion to be complete.

The energy equation is applied to the perfect gas, according to the first principle of thermodynamics, this implies:

2.2.1. General equation of stoichiometric reaction

In Eq. (7), the first part refers to the reactants and the second part refers to the products.

$$CH_4 + C_2H_6 + \alpha * a * (O_2 + 3.76N_2) \rightarrow b * CO_2 + c * H_2O + d * N_2 + e * O_2 \tag{7}$$

CH_4, C_2H_6: are the methane and ethane moles, respectively, in the natural gas composition, α is excess air, $(O_2 + 3.76N_2)$ is the is the composition of air for complete combustion, CO_2, H_2O, N_2, O_2 are the products obtained after combustion and (a, b, c, d, e) are the indices for obtaining the stoichiometric equilibrium.

2.2.2. Stoichiometric equation

Eq. (8), for the energy balance is translated, with the coefficients of the chemical Eq. (7), incorporating the values of Tab. 2 and Tab. 3 (Andrade *et al.*, 2007):

$$\Delta H_{C,CH_4,298} + \Delta H_{C,C_2H_6,298} + \int_{T_I}^{T_{I'}} \alpha * a * \left[C_{p,O_2} + 3{,}76 * C_{p,N_2}\right] dT = \int_{T_I}^{T_F} \left[b * C_{p,CO_2} + c * C_{p,H_2O} + d * C_{p,N_2} + e * C_{p,O_2}\right] dT \quad (8)$$

$\Delta H_{C,CH_4,298}$ and $\Delta H_{C,C_2H_6,298}$ are the methane and ethane combustion enthalpies respectively and $C_{p,CO_2}, C_{p,H_2O}, C_{p,N_2}$ and C_{p,O_2} are the specific heat at constant pressure.

The values of the reactants and the products can be found from the stoichiometric reaction equation. Therefore, the only variable to be determined in Eq. (8) is the adiabatic flame temperature T_F.

2.2.3. Thermodynamic properties in the determination of adiabatic flame temperature

The parameters required for the calculation of the adiabatic flame temperature are presented in Tab. 2 and Tab. 3:

Table 2. Specific heat at constant pressure of some substances for the determination of adiabatic flame temperature (Perry *et al.*, 1973; Sonntag *et al.*, 1998)

Substância	Cp (cal/mol K)	Intervalo (K)
CO_2 (g)	$-0{,}8929+0{,}7297T^{1/2}+-9{,}807x10^{-3}T+5{,}784x10^{-7}T^2$	300-3500
H_2O (g)	$8{,}22+0{,}00015T+0{,}00000134T^2$	300-2500
N_2 (g)	$6{,}50+0{,}00100T$	300-3000
O_2 (g)	$8{,}27+0{,}000258T-187700/T^2$	300-5000

Table 3. Enthalpy of combustion of methane and ethane (Perry *et al.*, 1973).

Substância	PCS (cal/mol)	PCS (cal/g)	PCI (cal/mol)	PCI (cal/g)
Metano, CH_4 (g)	212798	13265	191759	11954
Etano, C_2H_6 (g)	372820	12399	341261	11350

3. RESULTS AND DISCUSSIONS

3.1. Development of the proposed mathematical model

Knowing the input variables, as shown in Tab. 1, the adiabatic flame temperature is obtained from the *Gaseq software* using the compositions of the respective gases. An approximation of these flame temperatures of each case can be determined by making use of the stoichiometric reaction shown in Eqs. (7) and (8), and the thermodynamic properties shown in Tab. 2 and Tab. 3. The factorial experiment tool 2^3 establishes that with 3 input variables we must perform 8 experiments.

The experiments developed are shown in Tab. 4, in which a change was made with the signs (-1) and (+1) trying not to repeat any lines so that the 8 experiments are different.

The variables A, B and C represent the concentration of methane (%) in fuel, excess air (%) and air temperature (K), respectively. The average adiabatic flame temperature of the 8 experiments shown is 2064,32.

Table 4. Determination of adiabatic flame temperature based on preliminary variables

A CH_4 (%)	B α (%)	C T_{air} (K)	Adiabatic flame temperature (Gaseq) T_{af} (K)
-1	-1	-1	2109,22
+1	-1	-1	2097,36
-1	+1	-1	1624,83
+1	+1	-1	1616,97
-1	-1	+1	2503,19
+1	-1	+1	2467,31
-1	+1	+1	2051,97
+1	+1	+1	2043,72

Given the adiabatic flame temperature values for each case, the first, second and third order effects are calculated using Eq. (1), and the results are shown in Tab. 5.

Table 5. Effects of adiabatic flame temperature parameter factors

E	$\bar{Y}$ (+)	$\bar{Y}$ (-)	Effects
E_A	2056,340	2072,303	-15,963
E_B	1834,373	2294,270	-459,898
E_C	2266,548	1862,095	404,453
E_{AB}	2068,275	2060,368	7,907
E_{AC}	2061,270	2067,373	-6,102
E_{BC}	2075,568	2053,075	22,492
E_{ABC}	2067,275	2061,368	5,908

From Tab. 5, the best fit occurs when we have the following relationship between the variables A (-), B (-) and C (+), which means that to obtain the maximum adiabatic flame temperature, the methane concentration should be adjusted to 70%, excess air at 20% and air temperature at 873K. With the obtained effects, we determined the global variance without replicates and the experimental error through Eqs. (2) and (3), respectively. The overall non-replicating variance ($S_P{}^2$) is 34.90 and the experimental error (S_P) is 5.91.

Significance tests are determined with Eq. (4), the values of the effects presented in Tab. 5 and the experimental error, the results are presented in Tab. 6.

Table 6. Significance test of adiabatic flame temperature parameters

Teste de significância						
t_A	t_B	t_C	t_{AB}	t_{AC}	t_{BC}	t_{ABC}
2,70(1)	77,85(1)	68,46(1)	1,34	1,03	3,81(1)	1,00

(1) Significant tests that present a higher value in relation to the critical test (2.12) determined with a degree of freedom of 16 and a level of significance of 95%.

The second order significant test, BC, will be evaluated by the interaction graph Fig. 1, to identify and/or discard the relationship between the two variables.

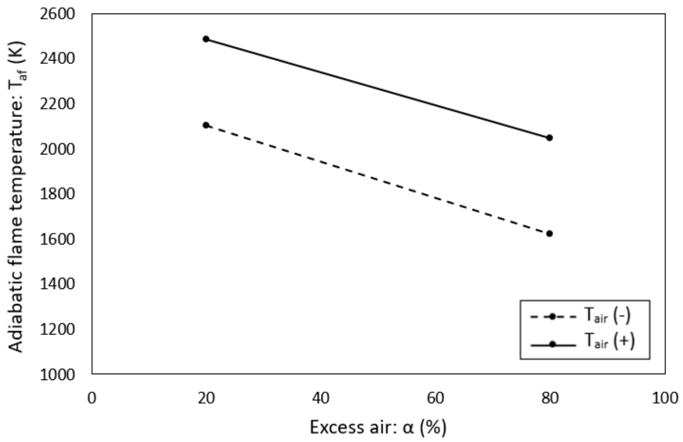

Figure. 1. Discard the interaction between excess air (α) and air temperature (T_{air}). Variables B-C.

By discarding the interaction between excess air (α) and air temperature (T_{air}), we encode each input variable as shown in Eq. (5). The values of a, b, and c must be between -1 and 1.

$$a = \frac{\text{CH4}-80}{10} \tag{9}$$

CH_4: methane concentration (%), ranges from [70-90]

$$b = \frac{\alpha-50}{30} \tag{10}$$

α: excess air (%), ranges from [20-80]

$$c = \frac{\text{Tair}-585,5}{287,5} \tag{11}$$

T_{air}: air temperature (K), ranges from [298-873]

We develop the mathematical model following the sequence of Eq. (6). For this, 8 experiments were considered, varying the maximum and minimum values of the presented variables, such as: methane concentration (%), air excess (%) and air temperature (K).

Adiabatic flame temperatures were determined in the stoichiometric composition with *Gaseq software* and the proposed mathematical model. The complete tool of factorial experiments 2^3 was used to obtain the correlation shown in Eq. (12) below.

$$T_{ac} = 2064{,}321 - \frac{15{,}963}{2}(a) - \frac{459{,}898}{2}(b) + \frac{404{,}453}{2}(c) + \frac{7{,}907}{2}(ab) - \frac{6{,}102}{2}(ac) + \frac{22{,}492}{2}(bc) + \frac{5{,}908}{2}(abc) \tag{12}$$

3.2. Validation of the model for the combustion of natural gas

The model will be tested with results obtained with the *Gaseq* chemical balance *software*, developed by Morley, which can be downloaded free of charge at http://www.c.morley.dsl.pipex.com/. In the references, the software is quoted using the author's name. This software uses a Gibbs energy minimization routine to establish equilibrium conditions in the combustion process. Figure 2 shows the results of the adiabatic flame temperature obtained by Eq. (12), by stoichiometric combustion of the natural gas at constant pressure. As you can see, there is a good fit with the data using the *Gaseq software* presented in Tab. 4. The validation of the model was determined in terms of the square correlation coefficient (R^2).

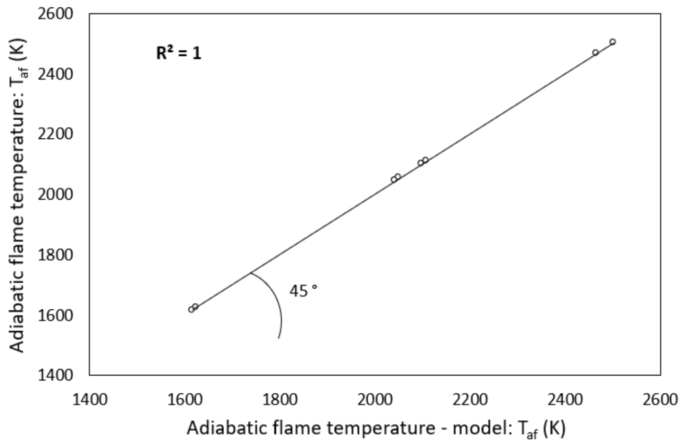

Figure 2. Validation of the mathematical model in terms of the square correlation coefficient (R^2) for the determination of adiabatic flame temperature in the combustion of natural gas at constant pressure.

3.3. Results of simulations of the model for the combustion of natural gas in the reheating furnace as a function of factors: CH_4, α and T_{air}

We developed three cases using the mathematical model obtained in Eq. (12) with the purpose of presenting an adiabatic flame temperature distribution and determining the maximum temperature reached in the combustion of natural gas. In each case, two of the three initial variables will be varied (methane concentration, excess air and air temperature) and the third constant variable will be maintained in each case.

3.3.1. Case 1. Simulation of adiabatic flame temperature in relation to methane concentration

The adiabatic flame temperature was determined based on the methane concentration, ranging from 70% to 90%, normally used in industrial furnaces (Denev *et al.*, 2017).

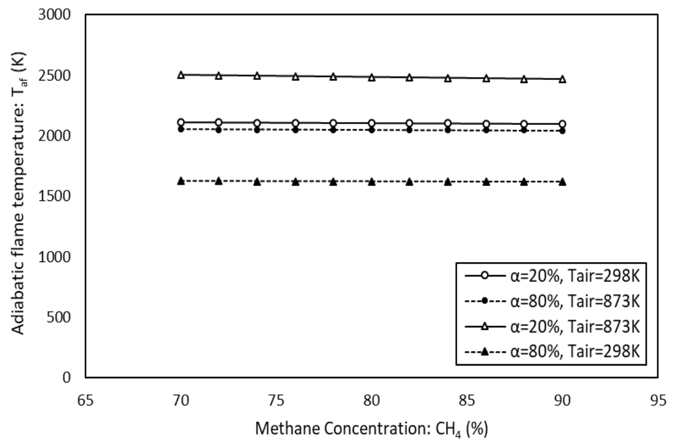

Figure 3. Simulation of the adiabatic flame temperature in the combustion of natural gas at constant pressure in relation to methane concentration (%), with variation of: α: excess air 20% - 80% and T_{air}: air temperature 298K - 873K.

Figure 3, four determining processes are observed to obtain the adiabatic flame temperature. In that the third process shows us the maximum adiabatic flame temperature reached in the combustion of the natural gas, which occurs when the excess air is as small as possible, in this case it is 20%, and the air must be preheated to a temperature of 873K, however, it is appreciated that with increasing methane concentration in the fuel, the flame temperature remains almost constant.

3.3.2. Case 2. Simulation of adiabatic flame temperature in relation to excess air

The adiabatic flame temperature was determined based on excess air, ranging from 20% to 80%, normally used in industrial furnaces (Caillat, 2017).

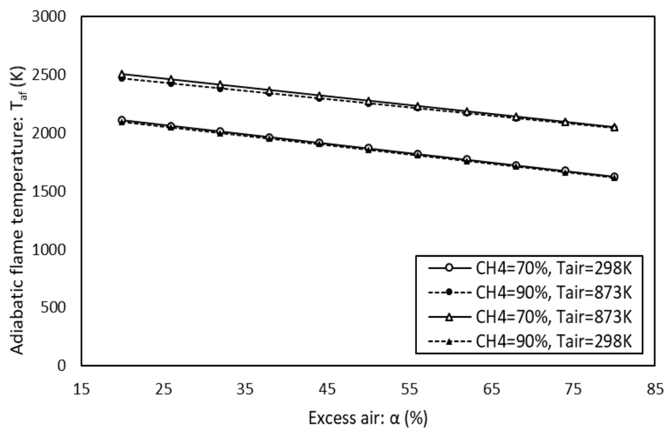

Figure 4. Simulation of the adiabatic flame temperature in the combustion of natural gas at constant pressure in relation to excess air (α), with variation of: CH_4: methane concentration 70% - 90% and T_{air}: air temperature 298K - 873K.

Figure 4, four determining processes are observed to obtain the adiabatic flame temperature. In that the third process shows us the maximum adiabatic flame temperature reached in the combustion of natural gas, which occurs when the percentage of methane-ethane varies from 70% - 30%, respectively, and the air must be preheated to a temperature of 873K, however, it is appreciated that with increasing excess air, the flame temperature is reduced. The function of excess air is to control the temperature of the flame in the combustion process and produce the most complete combustion possible.

3.3.3. Case 3. Simulation of adiabatic flame temperature in relation to air temperature

The adiabatic flame temperature was determined based on the air temperature, ranging from 298K to 873K, normally used in industrial furnaces (Caillat, 2017).

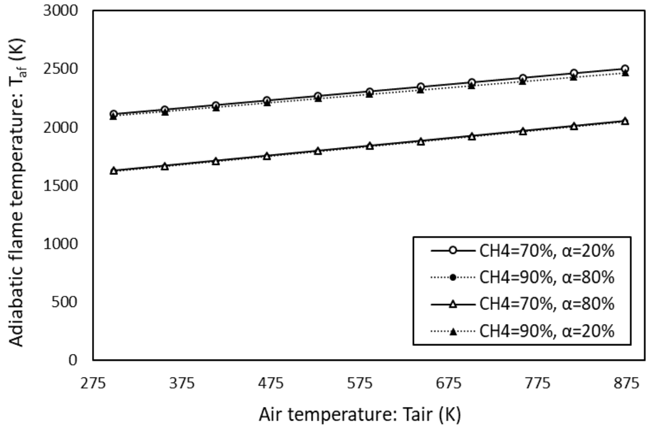

Figure 5. Simulation of the adiabatic flame temperature in the combustion of natural gas at constant pressure in relation to air temperature (T_{air}), with variation of CH_4: methane concentration 70% - 90% and α: air excess 20% - 80%.

Figure 5, four determining processes are observed to obtain the adiabatic flame temperature. In that the first process shows us the maximum adiabatic flame temperature reached in the combustion of natural gas, which occurs when the percentage of methane-ethane varies from 70% - 30%, respectively, and the excess air is 20%, however , it is appreciated that with the preheating of the air temperature, the temperature of the flame increases. The function of preheating the air is to increase the heat transfer rates, improve the efficiency of the combustion process, increase the flame temperature and the stability of the furnace.

The results obtained show the effectiveness of the mathematical model presented in Eq. (12) and corroborated by the coefficient of correlation to the square (R^2) equal to 1, shown in Fig. 2. Through this comparison, it is demonstrated the similarity of the results with those obtained through the stoichiometric reaction of natural gas.

The model was tested through three cases to determine the maximum adiabatic flame temperature, obtaining the following results:

The maximum adiabatic flame temperature can be reached when: in case A, the excess air is as small as possible 20% and the air is preheated to 873K; in case B, the methane concentration in the fuel preparation is 70% and the air is preheated to 873K; and in case C, the methane concentration in the fuel preparation is 70% and the excess air is 20%.

The advantage of using the mathematical model is to obtain the adiabatic flame temperature in a shorter time, varying only 3 parameters and entering them into the Eq. (12). Unlike the *Gaseq software*, which in order to obtain the adiabatic flame temperature requires describing the complete composition of the fuel. In this case, we have a methane composition that varies from 70% to 90%, since the percentages of the mixture with ethane also influence the composition, which means that if 80% methane is needed, the entire fuel composition It changes and the parameters in the software must be filled again. This makes work heavier and slower. The model proposes to save time and present the temperature behavior of the adiabatic flame through 3 parameters that vary between its lower and upper limits, as shown in Tab. 1.

4. CONCLUSIONS

The mathematical model for the determination of adiabatic flame temperature was developed and validated based on the square correlation coefficient (R^2), which is equal to 1; in the same way, the model can be used with the variation of the parameters established in each independent variable.

In order to obtain the highest adiabatic flame temperature, only the parameters of the independent variables presented in this paper are varied, it is recommended that the methane concentration in the fuel preparation is 70%, the air excess is as low as 20% and that the air is preheated until it reaches the maximum temperature, in this case 873K.

Through the presented model, it is sought to obtain the ideal flame temperature required by the materials that receive the heat treatment in the reheating furnace, varying the parameters of the input variables and, therefore, making decisions in the shortest possible time for the benefit of the industry.

A recommendation for future work is that the methodology to obtain the proposed mathematical model can be used with various types of fuels. The most used in the steel industry like the gas from coke oven (COG), blast furnace (BFG) and steel mill (LDG). These types of fuels have many variations in their composition, sometimes it has 12 to 15 components, and its variation is complicated when there are mixtures between them. By developing the mathematical model with the proposed methodology, we can obtain the flame temperature for many different scenarios only three parameters. In this way we can save time, since we avoid the work of filling in all the data of the compositions in the software and modifying them for each mixture.

5. ACKNOWLEDGEMENTS

The authors are grateful to FAPESP (Fundação de Amparo à Pesquisa do Estado de São Paulo) for support of this work through Project 2017/08975-1.

6. REFERENCES

Alves, P.C., Da Rocha, V.C., Pereira, J.A.M., Bielefeldt, W.V., Vilela, A.C.F., 2018. "Review and planning of experiments with steel and slag in laboratory furnace". *Journal of Materials Research and Technology*. Vol. 7, No. 1, pp. 387–394.

An, R., Yu, B., Li, R., Wei, Y.M., 2018. "Potential of energy savings and CO2 emission reduction in China's iron and steel industry". *Applied Energy*. Vol. 226, No. 1, pp. 862–880.

Andrade, C.J., McQuay, M.Q., 2007. *Princípios de combustão aplicada*, Ufsc, Brasil, 1st edition.

Andreas, S., 2011. "Feedback tracking control of continous reheating furnaces", *The International Federation of Automatic Control* - IFAC, Italy.

Barmatov, E., Hughes, T.L., 2017. "Effect of corrosion products and turbulent flow on inhibition efficiency of propargyl alcohol on AISI 1018 mild carbon steel in 4 M hydrochloric acid". *Corrosion Science*. Vol. 123, No. 1, pp. 170–181.

Caillat, S., 2017. "Burners in the steel industry: Utilization of by-product combustion gases in reheating furnaces and annealing lines". *Energy Procedia*. Vol. 120, No. 1, pp. 20–27.

Casal, J.M., Porteiro, J., Míguez, J.L., Vázquez, A., 2015. "New methodology for CFD three-dimensional simulation of a walking beam type reheating furnace in steady state". *Applied Thermal Engineering*. Vol. 86, No. 1, pp. 69–80.

Chen, D., Lu, B., Dai, F.Q., Chen, G., Yu, W., 2018. "Variations on billet gas consumption intensity of reheating furnace in different production states". *Applied Thermal Engineering*. Vol. 129, No. 1, pp. 1058–1067.

Chun, T., Long, H., Di, Z., Zhang, X., Wu, X., Qian, L., 2017. "Novel technology of reducing SO2 emission in the iron ore sintering". *Process Safety and Environmental Protection*. Vol. 105, No. 1, pp. 297–302.

Denev, J.A., Dinkov, I., Bockhorn, H., 2017. "Burner design for an industrial furnace for thermal post-combustion". *Energy Procedia*. Vol. 120, No. 1, pp. 484–491.

Emadi, A., Saboonchi, A., Taheri, M., Hassanpour, S., 2014. "Heating characteristics of billet in a walking hearth type reheating furnace". *Applied Thermal Engineering*. Vol. 63, No. 1, pp. 396–405.

Gan, M., Fan, X., Lv, W., Chen, X., Ji, Z., Jiang, T., Yu, Z., Zhou, Y., 2016. "Fuel pre-granulation for reducing NOx emissions from the iron ore sintering process, Powder Technology". *Powder Technology*. Vol. 301, No. 1, pp. 478–485.

Han, S.H., Chang, D., Huh, C., 2011. "Efficiency analysis of radiative slab heating in a walking-beam-type reheating furnace". *Energy* Vol. 36, No. 1, pp. 1265–1272.

Hindasageri, V., Vedula, R.P., Prabhu, S. V., 2014. "A novel method of estimation of adiabatic wall temperature for impinging premixed flame jets". *International Journal of Heat and Mass Transfer*. Vol. 77, No. 1, pp. 185–193.

Husmann, T., Magnus, C.S., 2016. "Thermography in incremental forming processes at elevated temperatures". *Measurement*. Vol. 77, No. 1, pp. 16–28.

Landfahrer, M., Prieler, R., Mayr, B., Gerhardter, H., Zmek, T., Klarner, J., Hochenauer, C., 2018. "Characterization of the temperature distribution on steel tubes for different operating conditions in a reheating furnace using CFD and three different measuring methods". *Applied Thermal Engineering*. Vol. 133, No. 1, pp. 39–48.

Lu, B., Chen, G., Chen, D., Yu, W., 2016. "An energy intensity optimization model for production system in iron and steel industry". *Applied Thermal Engineering*. Vol. 100, No. 1, pp. 285–295.

Ma, S.H., Wen, Z.G., Chen, J.N., Wen, Z.C., 2014. "Mode of circular economy in China's iron and steel industry: A case study in Wu'an city". *Journal of Cleaner Production journal*. Vol. 64, No. 1, pp. 505–512.

Montgomery, D.C., 2001. *Design and analysis of experiments*. John Wiley & Sons, USA, 5th edition.

Morley, C., *Gaseq: a chemical equilibrium program for windows*. Available at: <http://www.c.morley.dsl.pipex.com>

Oliveira, F.A.D., Carvalho, J.A., Sobrinho, P.M., de Castro, A., 2014. "Analysis of oxy-fuel combustion as an alternative to combustion with air in metal reheating furnaces". *Energy*. Vol. 78, No. 1, pp. 290–297.

Perry, R.E., Chilton, C.H., 1973. *Chemical Engineers' Handbook*. McGraw-Hill Book Company.

Rasul, M.G., Tanty, B.S., Mohanty, B., 2007. "Modelling and analysis of blast furnace performance for efficient utilization of energy". *Applied Thermal Engineering*. Vol. 27, No. 1, pp. 78–88.

Sonntag, R.E., Borgnakke, C., Van Wylen, G., 1998. *Fundamentos da termodinámica clássica*. Editora Edgard Blucher Ltda, 2th edition.

Stelzner, B., Weis, C., Habisreuther, P., Zarzalis, N., Trimis, D., 2017. "Super-adiabatic flame temperatures in premixed methane flames: A comparison between oxy-fuel and conventional air combustion". *Fuel*. Vol. 201, No. 1, pp. 148–155.

Strobel, R., Waldner, M.H., Gablinger, H., 2018. "Highly efficient combustion with low excess air in a modern energy-from-waste (EfW) plant". *Waste Management*. Vol. 73, No. 1, pp. 301–306.

Švantner, M., Vacíková, P., Honner, M., 2012. "IR thermography heat flux measurement in fire safety applications". *Infrared Physics and Technology*. Vol. 55, No. 1, pp. 292–298.

Wang, G., Mei, B., Liu, X., Zhang, G., Li, Y., Qi, F., 2018. "Investigation on spherically expanding flame temperature of n-butane/air mixtures with tunable diode laser absorption spectroscopy". *Proceedings of the Combustion Institute*. Vol. 5, No. 1, pp. 1–8.

Wu, M., Shu, G., Chen, R., Tian, H., Wang, X., Wang, Y., 2018. "A new model based on adiabatic flame temperature for evaluation of the upper flammable limit of alkane-air-CO2mixtures". *Journal of Hazardous Materials*. Vol. 344, No. 1, pp. 450–457.

Yang, J., Cai, J., Sun, W., Huang, J., 2017. "Optimal allocation of surplus gas and suitable capacity for buffer users in steel plant". *Applied Thermal Engineering*. Vol. 115, No. 1, pp. 586–596.

7. RESPONSIBILITY NOTICE

The authors are the only responsible for the printed material included in this paper.